Bonding Properties of the Water Dimer: A Comparative Study of Density Functional Theories

Xin Xu[†] and William A. Goddard, III*

Materials and Process Simulation Center (139-74), California Institute of Technology, Pasadena, California 91125

Received: June 30, 2003; In Final Form: December 9, 2003

For a variety of density functional theories, we examined the ground-state properties of the water monomer (geometry, vibrational frequencies, dipole moment, polarizability) and dimer (geometry, vibrational frequencies, bond energy, and barrier heights for the transition states for the interchange of hydrogen atoms within the dimer). Thus, we considered LDA (SVWN), seven pure GGA methods (BLYP, BP86, BPW91, PWPW, mPWPW, PBEPBE, and XLYP), and eight hybrid GGA methods (BH&HLYP, B3LYP, B3P86, B3PW91, PW1PW, mPW1PW, PBE1PBE and X3LYP). We find that the best overall performance is given by X3LYP, a hybrid method using a modified GGA constructed from a linear combination of the Becke and Perdew GGAs. Comparing with the exact values, the errors in X3LYP for the water dimer are 0.05 kcal/mol (bond energy), 0.004 Å (bond distance), and 12 cm⁻¹ (vibrational modes), and for the monomer, the errors are 0.002 Å (bond distance), 0.6° (bond angle), 14 cm⁻¹ (vibrational modes), 0.005 D (dipole moment), and 0.008 ų (polarizability). These data were not used in determining the parameters or form of X3LYP, suggesting that X3LYP should be generally useful for predicting accurate properties for systems dominated by hydrogen bonding, electrostatics, and van der Waals (dispersion) interactions, such as ligand/protein complexes.

1. Introduction

As the genomics revolution progresses to provide the structures for all of the proteins of life, there will be an opportunity for a new paradigm in virtual drug design in which each prospective drug is tested in silico against not only the target but also all of the other proteins of the body. To obtain sufficiently accurate calculated binding energies to be useful in drug design, it will be essential to develop computational methods accurate to 0.1 kcal/mol. Achieving this accuracy is an enormous challenge. Indeed, for a system as simple as the water dimer, achieving this level of accuracy requires ab initio calculations at the level of CCSD(T) theory with the basis set extrapolated to infinity. It is estimated that this leads to an uncertainty of ± 0.05 kcal/mol¹. Such extensive calculations are not likely to be practical on ligand-protein systems in the next few years; therefore, we seek a methodology that can yield such accuracy at a much more practical cost.

The current generation of methods based on density functional theory (DFT) $^{2-14}$ is likely to be practical for such systems, but the problem is that DFT methods are known to be poor at describing the London dispersion (van der Waals attraction) interactions that are so important in noncovalent bonding. Thus, the DFT methods based on the Becke-type functionals^{6,7} lead to completely repulsive interactions for noble gas dimers, 2,15,16 but the DFT methods based on the Perdew-type functionals⁸ lead to interactions of noble gas dimers (He₂ and Ne₂) that are several times too large. 2,12 These dispersion interactions constitute \sim 20% of the cohesive energy of liquid water, making this increased accuracy essential. 17

Recently, we developed the X3LYP extended functional² for DFT to improve the accuracy for van der Waals complexes (where London dispersion forces play an essential role) significantly while also improving the accuracy of the heats of formation, ionization potentials, electron affinities, and total atomic energies over that of the most popular and accurate theory, B3LYP. In this work, we test how well the X3LYP functional describes the most important hydrogen-bonded system, the water dimer. Here we examine the binding energy, geometry, and vibrational frequencies of the dimer as well as the transition states (barrier and geometry) for the interchange of hydrogen atoms within the dimer. We also present the results for the monomer (geometry, vibrational frequencies, dipole moment, and polarizabilities). To compare with other methods, we also carried out calculations for these same quantities using Hartree-Fock (HF), the local density approximation (LDA), and 15 other flavors of generalized gradient approximation (GGA) with and without using some component of exact exchange.2-14

We find that X3LYP leads to the best overall properties of these systems, with a bond energy of the dimer accurate to 0.05 kcal/mol and an O-O bond distance accurate to 0.004 Å. This suggests that X3LYP can provide the level of accuracy required for ligand-protein interactions.

Section 2 presents the computational details, and section 3 presents the results and discussion. Finally, section 4 presents the conclusions.

2. Computational Details

Table 1 summarizes the 16 flavors of DFT methods examined in the present work. The SVWN functional, used for carrying out LDA calculations, combines the Slater exchange functional³

^{*} To whom correspondence should be addressed. E-mail: wag@wag.caltech.edu.

[†] On sabbatical leave from Xiamen University, China.

TABLE 1: Summary of the DFT Equations Examined in the Present Work.

DFT name	equation
	LDA
SVWN	$1.0E_x(Slater) + 1.0E_c(VWN)$
	GGA
BLYP	$1.0E_x(\text{Slater}) + 1.0\Delta E_x(\text{B88}) + 1.0E_c(\text{LYP})$
BP86	$1.0E_x(\text{Slater}) + 1.0\Delta E_x(\text{B88}) + 1.0E_c(\text{PZ81,local}) + 1.0\Delta E_c(\text{P86,nonlocal})$
BPW91	$1.0E_x(\text{Slater}) + 1.0\Delta E_x(\text{B88}) + 1.0E_c(\text{PW91})$
PWPW	$1.0E_x(\text{Slater}) + 1.0\Delta E_x(\text{PW91}) + 1.0E_c(\text{PW91})$
mPWPW	$1.0E_x(\text{Slater}) + 1.0\Delta E_x(\text{mPW}) + 1.0E_c(\text{PW91})$
PBEPBE	$1.0E_x(Slater) + 1.0\Delta E_x(PBE) + 1.0E_c(PW91,local) + 1.0\Delta E_c(PBE,nonlocal)$
XLYP	$1.0E_x(\text{Slater}) + 0.722\Delta E_x(\text{B88}) + 0.347\Delta E_x(\text{PW91}) + 1.0E_c(\text{LYP})$
	Hybrid Methods
BH&HLYP	$0.50E_x(HF) + 0.50E_x(Slater) + 0.50\Delta E_x(B88) + 1.0E_c(LYP)$
B3LYP	$0.20E_x(HF) + 0.80E_x(Slater) + 0.72\Delta E_x(B88) + 0.19E_c(VWN) + 0.81E_c(LYP)$
B3P86	$0.20E_x(HF) + 0.80E_x(Slater) + 0.72\Delta E_x(B88) + 1.0E_c(VWN) + 0.81\Delta E_c(P86)$
B3PW91	$0.20E_x(HF) + 0.80E_x(Slater) + 0.72\Delta E_x(B88) + 1.0E_c(PW91,local) + 0.81\Delta E_c(PW91,nonlocal)$
PW1PW	$0.25E_x(HF) + 0.75E_x(Slater) + 0.75\Delta E_x(PW91) + 1.0E_c(PW91)$
mPW1PW	$0.25E_x(HF) + 0.75E_x(Slater) + 0.75\Delta E_x(mPW91) + 1.0E_c(PW91)$
PBE1PBE	$0.25E_x(HF) + 0.75E_x(Slater) + 0.75\Delta E_x(PBE) + 1.0E_c(PW91,local) + 1.0\Delta E_c(PBE,nonlocal)$
X3LYP	$0.218E_x(\text{HF}) + 0.782E_x(\text{Slater}) + 0.542\Delta E_x(\text{B88}) + 0.167\Delta E_x(\text{PW91}) + 0.129E_c(\text{VWN}) + 0.871E_c(\text{LYP})$

with the correlation of the homogeneous electron gas in the random phase approximation by Vosko, Wilk, and Nusair.⁴ We consider seven pure GGA methods (BLYP,^{5,7} BP86,^{7–9} BPW91,^{7,11} PWPW,^{10,11} mPWPW,^{11,12} PBEPBE,^{11,13} and XL-YP^{2,5}) and eight hybrid GGA methods (BH&HLYP,^{5–7} B3LYP,^{4–7} B3P86^{4–7}, B3PW91^{6,7,11}, PW1PW,^{10–12} PBE1-PBE,^{11,13,14} and X3LYP^{2–6,10}).

The most popular flavor of DFT for finite systems is B3LYP, ³⁻⁷ a hybrid GGA formed by combining the correlation functionals of VWN⁴ and Lee-Yang-Parr (LYP⁵) and a mixed exchange functional of three terms: ⁶ a portion of exact exchange, Slater local exchange, ³ and the nonlocal gradient correction of Becke88. ⁷

X3LYP extends this Becke three-parameter scheme by replacing the Becke88 functional with a linear combination of the Becke88 and PW91 exchange functionals.^{7,10} Thus the F^X(s) function for the extended exchange functional is written as

$$F^{X}(s) = 1 + a_{x1}(F^{B88}(s) - 1) + a_{x2}(F^{PW91}(s) - 1)$$
 (1)

where the mixing parameters $\{a_{x1}, a_{x2}\} = \{0.722, 0.347\}$ were determined through a least-squares fitting to the total energies of 10 atoms, the ionization potentials for 16 atoms, the electron affinities for 10 atoms, and the atomization energies for 38 molecules selected to represent the important chemistry for the first- and second-row elements (including open- and closed-shell molecules; molecules with single, double, and triple bonds; ionic systems; and systems requiring multiple determinants for proper descriptions).² In particular, we included He₂ and Ne₂ as representative van der Waals systems (but did not include any data about the water dimer). The mixing coefficients of X3LYP as well as XLYP (a pure GGA) can be found in Table 1.

All of the DFT calculations were carried out using the implementation in Jaguar. ¹⁸ The exchange—correlation integrals were evaluated using a pruned (90, 434) grid, which has 90 radial shells and a full set of 434 angular points that vary with the radial coordinate.

The aug-cc-pVTZ(-f) basis sets were used on all atoms, and a full geometry optimization was carried out for all stable complexes and saddle points. ^{19,20} Because the potential energy surfaces for the water dimer are very flat, the energies during all geometry optimizations were converged to \sim 5 μ hartree or better; the corresponding root-mean-square deviation of the

gradient of the energy with respect to the nuclear coordinates was less than 0.00001 hartree/bohr.

Vibrational frequencies (from the analytic Hessian) were calculated to ensure that each minimum is a true local minimum (containing only positive frequencies) and that each transition state has only a single imaginary frequency (one negative eigenvalue of the Hessian).

Polarizabilities were calculated using a three-point finite field method with an electric field of 0.006 au.

It is generally accepted that basis set superposition error (BSSE) must be considered to obtain accurate calculations of the binding energy.^{21,22} Consequently, we applied the full counterpoise procedure in all calculations.²³

$$\Delta E(\text{BSSE, A-D}) = \\ E(A)_{A} - E(A)_{A-D} + E(D)_{D} - E(D)_{A-D}$$

where $E(A)_{A-D}$ and $E(A)_A$ represent the energy of A calculated using its geometry within the dimer and the basis functions of A plus D in the former and those of A alone in the latter. For all DFT methods applied here, we find that the BSSE correction is between 0.02 and 0.09 kcal/mol.

3. Results and Discussion

= 104.52° from Benedict et al.²⁵

3.1. Ground-State Properties of the Water Monomer. 3.1.1. Geometry. Table 2 summarizes the calculated and experimental results for various properties of the water monomer. The various experimental values of the OH bond length range from 0.957 to 0.959 Å, and the experimental H-O-H angle of the monomer ranges from 103.9 to 105.0°. ²⁵⁻²⁷ The most widely accepted numbers are OH = 0.9572 Å and \angle HOH

We consider adequate accuracy in the geometry to be 0.005 Å for the O-H bond and 1° for the H-O-H angle. Table 2 shows that X3LYP and all other hybrid methods (except BH&HLYP) lead to this level of accuracy.

The HF method leads to a bond too short by 0.016 Å and a H-O-H angle too large by 1.7°, showing the importance of electron correlation. LDA (SVWN) overcorrects the O-H bond length, becoming too long by 0.013 Å, and leads to a bond angle 0.5° too large. For the water monomer, the gradient correction in GGA does not improve the geometry predictions over those of LDA.

TABLE 2: Geometry (Å, deg) and Vibrational Frequencies (cm⁻¹) of the Water Monomer^a

	geom	etry	f	requenc	y	
	R(O-H)	∠HOH	ν_1	ν_2	ν_3	MAD^g
HF	0.941	106.2	4126	1756	4223	227.2
		LDA	A			
SVWN	0.970	104.9	3729	1560	3835	99.5
		GG	4			
BLYP	0.973	104.4	3659	1604	3758	134.0
BP86	0.970	104.2	3708	1606	3810	99.4
BPW91	0.970	104.1	3708	1609	3809	99.0
PWPW	0.970	104.2	3707	1602	3809	101.7
mPWPW	0.970	104.2	3706	1605	3808	101.3
PBEPBE	0.971	104.1	3702	1601	3804	105.3
XLYP	0.972	104.4	3658	1607	3756	134.0
		Hybrid M	ethods			
BH&HLYP	0.951	105.7	3967	1684	4066	98.0
B3LYP	0.962	105.0	3801	1636	3901	28.3
B3P86	0.960	104.8	3838	1638	3940	6.6
B3PW91	0.960	104.8	3837	1639	3938	6.1
PW1PW	0.958	104.9	3865	1647	3968	19.7
mPW1PW	0.958	104.8	3866	1646	3968	20.3
PBE1PBE	0.959	104.8	3862	1643	3965	19.0
X3LYP	0.961	105.1	3820	1640	3919	14.3
best ab initio b	0.959	104.2	3833	1659	3943	4.0
exptl	0.957^{c}	104.5^{c}	3832^{c}	1648 ^c	3943 ^c	
	0.959^d 0.959^e	105.0^d 103.9^e	3657 ^f	1595 ^f	3756 ^f	

 $^{\it a}$ In boldface are cases with errors of less than 0.005 Å, 0.6°, or 20 cm⁻¹. ^b Reference 24. CCSD(T)/TZ2P(f,d)+dif. ^c Geometric parameters and experimental harmonic frequencies (ν_e , cm⁻¹) taken from ref 25. ν_1 : symmetric O-H stretching; ν_2 : H-O-H bending; ν_3 : asymmetric O-H stretching. ^d Reference 26. ^e Reference 27. ^f Experimental anharmonic frequencies (v₀, cm⁻¹) taken from ref 28. g Mean absolute deviation from experimental harmonic frequencies.

3.1.2. Vibrational Frequencies. Table 2 lists the vibrational frequencies for the monomer. Here the experimental frequencies include the harmonic values²⁵ (v_e) (upper value) and the directly observed (anharmonic) frequencies (v_0) (lower value). To obtain an overall comparison of the calculated frequencies with the experimental harmonic frequencies, we report the mean absolute deviation (MAD in cm⁻¹).

The best ab initio methods lead to MAD = 4.0 cm^{-1} . The best DFT results are for B3PW91 and B3P86 with MAD = 6.1 and 6.6 cm⁻¹, respectively. Next best is X3LYP with MAD = 14.3 cm⁻¹. Generally, the hybrid methods (except BH&HLYP) give the best frequencies. With HF, the O-H stretching modes and H-O-H bending mode are \sim 7% too high, leading to MAD $= 237.2 \text{ cm}^{-1}$. LDA (SVWN) leads to MAD $= 99.5 \text{ cm}^{-1}$, with O-H modes \sim 3% too low and the H-O-H mode \sim 5% too low. These deviations are as expected from the errors in bond lengths. (A bond length that is too short makes the mode too stiff.) The GGA cases without exact exchange lead to errors $(MAD \approx 100 \text{ cm}^{-1})$ comparable to LDA, indicating the importance of including some exact exchange.

We consider the accuracy of 14 cm⁻¹ provided by X3LYP to be adequate.

3.1.3. Dipole Moment. Electrostatic interactions are an essential component of ligand-protein interactions. The experimental quantity providing the best measure of the electron distribution in a molecule is the dipole moment. Because the experimental moment is 1.854 D,²⁹ we consider an accuracy of 0.006 D to be adequate. The basis for this criterion is that a dipole of 0.006 D positioned 3 Å from a charge of 1.0 electron leads to an error in energy of 0.045 kcal/mol, within our energy

criterion. Table 3 shows that X3LYP, B3LYP, and B3PW91 all give this level of accuracy.

The largest error (0.092 D) is for HF, whereas LDA (SVWN) is high by just 0.014 D. All nonhybrid GGAs lead to too little charge polarity, with errors of 0.04 to 0.05 D.

3.1.4. Dipole Polarizability. The static electric polarizability is related to the ease of mixing an excited state into the ground state in response to an external electric field.³² From perturbation theory, the polarizability is inversely proportional to the excitation energies of the system, which can be expected to scale as $1/(\epsilon_{\text{HOMO}} - \epsilon_{\text{LUMO}})$ (the energy difference between the highest occupied molecular orbital and the lowest unoccupied dipoleallowed molecular orbital). Because the orbital energies are sensitive to the asymptotic behavior of the functional, we expect this behavior to affect the polarizability.

Table 2 includes two sets of experimental data of the polarizability of the water monomer, 1.470 ± 0.03^{30} and 1.427 \pm 0.03³¹ Å³, differing by 3%. These light-scattering measurements require some corrections to obtain purely static values for comparisons with the theory. Because removing from the experimental data the unwanted contributions from vibrational, rotational, or other effects generally decreases the experimental value, we chose the smaller one, 1.427 Å^3 , as our reference.

X3LYP leads to the best polarizabilities, with MAD = 0.008(0.6%). The other hybrid methods (except BH&HLYP) lead to errors of 0.015 to 0.020. HF underestimates the static polarizability by 15% (MAD = 0.212), and LDA(SVWN) overestimates the static polarizability by 7% (MAD = 0.097). (The longrange potential is not sufficiently attractive, making the HOMO energy too small.) The nonhybrid GGAs all lead to worse polarizability results than LDA gives.

3.2. Ground-State Properties of the Water Dimer. Our results for the optimal geometry, the harmonic frequency, and the binding energy of the water dimer are presented in Tables 4-6, which also include the experimental data³³⁻³⁸ and the best ab initio calculation results. 1,24 Figure 1 provides the definition of the geometrical parameters.

3.2.1. Binding Energy. The binding energy of the dimer is the most important property. 21,22,24,32,39-43 It has been difficult to obtain accurate experimental values because of the low concentration of dimers present in water vapor (around 1% at 373 K).³⁸ The widely accepted experimental value of the bond energy from the lowest vibrational level is $D_0 = 3.59 \pm 0.5$ kcal/mol from the measurement of the thermal conductivity of water vapor.³⁸ There is not sufficient experimental vibrational information to correct this value to obtain the De value from the bottom of the binding curve; however, using the vibrational frequencies from theory leads to $D_e = 5.44 \pm 0.7 \text{ kcal/mol.}^{38}$ Because of these experimental uncertainties, accurate ab initio theoretical calculations are critical for the water dimer.

The best ab initio calculations on the water dimer used the CCSD(T) theory (coupled cluster with single and double excitations plus estimates of triples) by Klopper et al. These calculations included the extrapolation of the basis set level to infinity, leading to $D_e = 5.02 \pm 0.05 \text{ kcal/mol},^1 \text{ which we will}$ take as our reference. A thorough survey of other theoretical results is in ref 1. With 6-311++G(3df,3pd), Frisch et al. estimated that the ranges of the binding energies lie within 3.4-3.8 for HF, 4.5-5.4 for MP2, 4.5-5.2 for MP3, and 4.6-5.3 kcal/mol for MP4.43

We use the aug-cc-pVTZ(-f) basis set. Previous studies⁴¹ concluded that f functions and higher on O and d functions and higher on H make an ~ 0.1 kcal/mol net contribution to the binding energy of the water dimer.

TABLE 3: Electrostatic Properties of the Water Monomer^a

	dipole	polarizability					
	μ	α_{xx}	α_{yy}	$lpha_{zz}$	α^b	MAD	
HF	1.946	1.132	1.314	1.199	1.215	0.212	
			LDA				
SVWN	1.868	1.467	1.590	1.515	1.524	0.097	
			GGA				
BLYP	1.810	1.507	1.630	1.547	1.561	0.134	
BP86	1.816	1.452	1.578	1.505	1.512	0.085	
BPW91	1.815	1.458	1.578	1.507	1.514	0.087	
PWPW	1.815	1.511	1.593	1.527	1.543	0.117	
mPWPW	1.817	1.498	1.583	1.518	1.533	0.106	
PBEPBE	1.813	1.507	1.594	1.526	1.542	0.115	
XLYP	1.805	1.515	1.636	1.552	1.568	0.141	
			Hybrid Methods				
BH&HLYP	1.899	1.245	1.393	1.302	1.314	0.114	
B3LYP	1.856	1.385	1.513	1.430	1.443	0.016	
B3P86	1.861	1.337	1.481	1.403	1.407	0.020	
B3PW91	1.859	1.343	1.482	1.405	1.410	0.017	
PW1PW	1.863	1.358	1.478	1.394	1.410	0.017	
mPW1PW	1.864	1.353	1.475	1.395	1.408	0.019	
PBE1PBE	1.862	1.357	1.480	1.398	1.412	0.015	
X3LYP	1.859	1.367	1.500	1.415	1.427	0.008	
exptl	1.854 ^d	$egin{array}{l} {f 1.372} \pm {f 0.013}^c \ 1.415 \pm 0.013^f \end{array}$	$ \begin{array}{l} 1.483 \pm 0.013^{e} \\ 1.528 \pm 0.013^{f} \end{array} $	$ 1.426 \pm 0.003^{e} \\ 1.468 \pm 0.013^{f} $	$egin{array}{l} {f 1.427} \pm {f 0.03}^e \ 1.470 \pm 0.03^f \end{array}$		

^a Dipole moment is in debye. Polarizability is in Å³. In boldface are cases with errors of less than 0.006 D or 0.014 Å³. ^b Isotropic polarizability $\alpha = \frac{1}{3}(\alpha_{xx} + \alpha_{yy} + \alpha_{zz})$. ^c Mean absolute deviation for polarizability. Data in ref 31 are taken as the reference. ^d Reference 29. ^e Reference 31. ^f Reference 30.

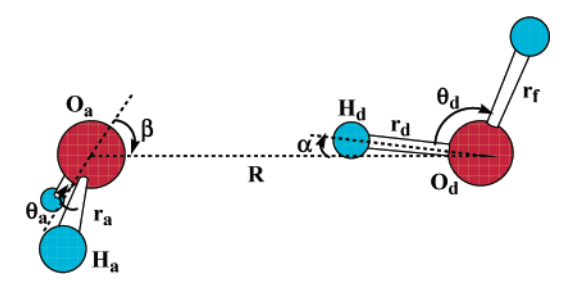


Figure 1. Bonding geometry of the ground-state water dimer.

The lowest errors in D_e are 0.04 kcal/mol (PBE1PBE), 0.05 (X3LYP), and 0.09 (BH&HLYP), all weaker than the exact value. The other hybrid methods lead to errors of 0.2 to 1.0 kcal/mol, and the pure GGA methods lead to errors of 0.1 to 1.6 kcal/mol. HF leads to an error of 1.3 kcal/mol too weak, and LDA (SVWN) leads to an error of 4.00 kcal/mol too strong! This error in LDA is probably the result of of its very poor description of London dispersion (leading to a bond energy for He₂ that is 11 times too strong²).

3.2.2. Geometry. 3.2.2a. $R_e(O-O)$. After the energy, the next most important property of the water dimer is the O-O distance. Determining an accurate experimental value for $R_e(O-O)$ has proven to be difficult.³³ Radio frequency and microwave spectra for various isotopically substituted water dimers have been studied by molecular beam electric resonance spectroscopy. The microwave spectra have been analyzed with a rigid rotator model to obtain structural information. The vibrationally averaged R_0 was determined to be 2.976 Å, from which it was estimated that $R_e = 2.946$ Å after correcting for anharmonicity.³³ However, the extreme floppiness of the water dimer makes these corrections uncertain.

The best ab initio value of $R_e(O-O) = 2.912$ Å was determined using CCSD(T)(Full) with basis sets extrapolated to infinity.¹ This is 0.034 Å shorter than the experimental value, leading some authors to question the experimental results.^{22,42} It is likely that to adjust R_0 to R_e requires correcting for zero-

point motion associated with the dimer's bending mode in addition to the anharmonicity of the O···O vibration. Thus, we consider 2.912 Å to be the exact value for comparing the various methods.^{22,42}

Many other theoretical studies of the interoxygen separation, $R_{\rm e}({\rm O-O})$, in the water dimer have been reported. $^{21,22,24,32,39-43}$ HF calculations by Frisch et al. reported values for $R_{\rm e}({\rm O-O})$ ranging from 2.971 Å with 6-31G(d) to 3.026 Å with 6-311++G(3df,3pd). 43 We obtain an HF value of $R_{\rm e}({\rm O-O})$ = 3.048 Å using aug-cc-pVTZ(-f). This is 0.136 Å longer than the best ab initio value [(CCSD(T)(FULL)^1] of 2.912 Å.

The best predictions of $R_e(O-O)$ for DFT methods are with mPWPW and X3LYP, which lead to values 0.001 and 0.004 Å shorter, respectively, than the best ab initio value.

LDA(SVWN) leads to $R_e(O-O) = 2.710$ Å, which is 0.202 too short! This is probably due to the poor description of dispersion. (For He₂, LDA² leads to a bond distance that is 0.2 Å too short.) The various nonhybrid GGA methods significantly improve the accuracy in $R_e(O-O)$, leading to an average error of 0.025 Å, ranging from 0.001 to 0.04 Å (too short). The eight flavors of hybrid methods examined here reduce the error further to 0.016 Å.

3.2.2b. Elongation of the O–H Bond. The elongation of the O–H bond in the donor water is also of interest.^{24,44} The best ab initio estimate of Δr_d (O–H) = 0.006 Å (longer) is based on CCSD(T)/TZ2P(f,d)+dif from Tschumper et al.²⁴

The best results are for X3LYP and BH&HLYP, which lead to $\Delta r_d(O-H)=0.007$ Å, within 0.001 Å of the best ab initio value.

The other hybrid methods also lead to errors in $\Delta r_{\rm d}({\rm O-H})$ of less than 0.003 Å. Among nonhybrid GGAs, the best are BLYP and XLYP, giving $\Delta r_{\rm d}({\rm O-H}) = 0.008$ Å with an error of 0.002 Å.

HF and LDA(SVWN) lead to $\Delta r_d(O-H) = 0.008$ (short) and 0.019 Å (long), respectively. The value for $r_d(O-H)$ is too short by 0.019 for HF and too long by 0.025 for LDA.

TABLE 4: Geometric Properties (Å, deg) for the Water Dimer^a

	R	$r_{ m d}$	$r_{ m f}$	$r_{\rm a}$	$ heta_{ ext{d}}$	$ heta_{ m a}$	α	β
HF	3.048	0.945	0.941	0.942	106.3	106.4	4.1	49.2
			LDA					
SVWN	2.710	0.989	0.969	0.972	105.7	105.3	7.2	71.9
			GGA					
BLYP	2.952	0.981	0.971	0.973	104.8	104.7	5.9	62.4
BP86	2.889	0.980	0.969	0.971	104.5	104.4	6.1	66.5
BPW91	2.946	0.979	0.969	0.971	104.4	104.4	5.3	63.9
PWPW	2.886	0.981	0.969	0.971	104.7	104.6	6.3	65.8
mPWPW	2.911	0.980	0.969	0.971	104.5	104.5	6.1	66.0
PBEPBE	2.899	0.981	0.970	0.972	104.5	104.5	6.3	66.2
XLYP	2.953	0.980	0.971	0.974	105.0	104.7	6.5	63.6
			Hybrid Met	nods				
BH&HLYP	2.905	0.958	0.950	0.952	106.0	105.9	5.7	57.1
B3LYP	2.926	0.970	0.961	0.963	105.4	105.3	5.8	60.0
B3P86	2.878	0.970	0.959	0.961	105.1	105.2	5.4	62.1
B3PW91	2.923	0.969	0.959	0.961	105.1	105.1	5.6	61.7
PW1PW	2.884	0.967	0.957	0.959	105.3	105.2	5.9	61.9
mPW1PW	2.898	0.967	0.957	0.959	105.1	105.2	5.7	62.4
PBE1PBE	2.896	0.968	0.958	0.960	105.1	105.1	5.9	61.9
X3LYP	2.908	0.968	0.959	0.961	105.6	105.5	5.9	59.6
best ab initio ^b	2.912	0.964	0.957	0.958	104.8	104.9	5.5	56.6
exptl ^c	2.976(+0.000, -0.030)						6 ± 20	57 ± 1

^a In boldface are cases with errors of less than 0.006 Å or 1°. ^b Reference 1, CCSD(T)(FULL)/IO275 → ∞ (IO275: interaction optimized basis set with 275 basis functions for the H₂O dimer. O: 7s5p5d3f2g1h; H_d: 2s4p1d, H: 2s3p, BF: 3s3p2d1f). c Reference 33.

TABLE 5: Vibrational Frequencies (cm⁻¹)^a of the Water Dimer Calculated with Various Flavors of DFT Methods

	ν_1	ν_2	ν_3	$ u_4$	ν_5	ν_6	MAD_1^{e}	ν_7	ν_8	ν_9	ν_{10}	ν_{11}	ν_{12}	MAD_2^f
HF	4214	4203	4119	4077	1775	1759	255.1	559	319	156	141	129	118	36.8
	LDA													
SVWN	3809	3802	3710	3418	1586	1562	121.7	795	476	275	205	178	153	73.0
	GGA													
BLYP	3748	3729	3653	3526	1621	1604	122.7	621	372	192	163	156	130	5.2
BP86	3797	3778	3700	3538	1626	1608	95.2	657	399	211	173	165	135	14.5
BPW91	3799	3778	3701	3556	1629	1610	90.7	629	380	203	180	151	135	10.6
PWPW	3797	3778	3699	3530	1621	1603	98.2	666	403	210	175	171	144	21.0
mPWPW	3797	3777	3699	3542	1625	1606	95.2	647	389	200	171	161	131	9.3
PBEPBE	3795	3773	3695	3536	1621	1600	99.5	651	387	194	180	159	133	10.2
XLYP	3740	3731	3646	3539	1622	1609	121.7	612	374	204	180	159	143	14.3
						Hybrid M	ethods							
BH&HLYP	4053	4041	3958	3865	1706	1687	115.4	636	371	193	158	158	133	2.3
B3LYP	3889	3873	3794	3678	1656	1637	15.0	634	375	193	160	159	133	3.8
B3P86	3927	3910	3830	3683	1660	1639	24.6	664	393	206	173	164	136	15.6
B3PW91	3928	3910	3830	3702	1660	1640	21.3	637	380	196	167	154	133	9.0
PW1PW	3953	3936	3855	3709	1668	1649	30.2	675	420	217	191	181	170	35.2
mPW1PW	3956	3938	3857	3727	1668	1648	31.5	649	385	196	164	159	134	7.3
PBE1PBE	3952	3935	3853	3720	1665	1644	29.7	654	389	199	164	163	142	11.3
$X3LYP^g$	3908	3891	3813	3700	1660	1643	12.3	636	375	200	167	162	144	8.2
best ab inito ^b	3934	3914	3827	3750	1686	1661	25.8	640	369	191	158	154	131	0
$exptl^c$	3899	3881	3797	3718	1669	1653	0							
$exptl^d$	3714	3698	3626	3548	1618	1600		520	320	243		155		

^aν₁: asymmetric O-H stretching of acceptor water molecule; ν₂: asymmetric O-H stretching of donor water molecule; ν₃: symmetric O-H stretching of acceptor water molecule; ν_4 : symmetric O-H stretching of donor water molecule; ν_5 : H-O-H bending of donor water molecule; ν₆: H-O-H bending of acceptor water molecule; ν₇: out-of-plane H-bond shear; ν₈: in-plane H-bond shear; ν₉: in-plane H-bond bending; ν₁₀: H-bond stretching; ν₁₁: H-bond torsion; ν₁₂: out-of-plane H-bond bending. ^b Reference 24, CCSD(T)/TZ2P(f,d)+dif. ^c Harmonic experimental frequencies (ν_e) are taken from refs 34 and 35. ^d Anharmonic experimental values in parentheses (ν_e) are taken from refs 36 and 37. ^e Mean absolute deviation from experimental harmonic frequencies for the high-frequency modes $(\nu_1 - \nu_6)$. ^f Mean absolute deviation from the best ab initio harmonic frequencies for the low-frequency modes $(\nu_7 - \nu_{12})$. ^g In boldface are cases with errors of less than 20 cm⁻¹.

3.2.2c. Bending of the Acceptor H_2O from the O-H Bond. Another important parameter is the angle (β) between the O-O distance vector and the molecular plane of the proton-accepting monomer. The experimental value (Table 5) for β is 57 \pm 10°.33 The large error bar indicates the difficulty in experimentally making a complete structure determination.

The best ab initio number is 55.6° at the CCSD(T)(Full)/ IO275 $\rightarrow \infty$ level. It is known that β is sensitive both to the level of the treatment of the correlation effect and to the quality of the basis set.41

The best DFT results are 57.1° for BH&HLYP and 59.6° for X3LYP. The hybrid methods lead to an average of $\beta = 60.8^{\circ}$.

TABLE 6: Bonding Properties of the Water Dimer

	$\Delta R_{\rm e}({ m O-O})$ Å	$\Delta r_{\rm d}({ m O-H})$ Å	$\Delta \nu_{\rm d} ({ m O-H}) \ { m cm}^{-1}$	$D_{ m e}^g$ kcal/mol	D_0 kcal/mol
HF	0.136	0.004	-97	3.71	1.76
LDA(SVWN)	-0.202	0.019	-364	9.02	6.56
		GG	A		
BLYP	0.040	0.008	-182	4.18	2.07
BP86	-0.023	0.010	-221	4.47	2.27
BPW91	0.034	0.019	-202	3.60	1.45
PWPW	-0.026	0.011	-228	5.43	3.20
mPWPW	-0.001	0.010	-215	4.48	2.33
PBEPBE	-0.013	0.011	-217	5.11	2.95
XLYP	0.041	0.008	-168	4.42	2.25
		Hybrid M	lethods		
BH&HLYP	-0.007	0.007	-152	4.93	2.75
B3LYP	0.014	0.008	-173	4.57	2.42
B3P86	-0.034	0.010	-206	4.74	2.52
B3PW91	0.011	0.009	-185	4.03	1.87
PW1PW	-0.028	0.009	-208	5.23	2.85
mPW1PW	-0.014	0.009	-190	4.60	2.43
PBE1PBE	-0.016	0.009	-193	4.98	2.78
X3LYP	-0.004	0.007	-170	4.97	2.77
best ab initio	0.000^{b}	0.006^{c}	-138^{c}	5.02^{b}	2.81^{d}
exptl			-170^{e}	5.44 ± 0.7^{f}	3.59 ± 0.5

 a We consider the best ab initio to be the reference state. Here, $\Delta R_e(O-O)$ is the deviation from the reference. $\Delta r_d(O-H)$ and $\Delta \nu_d(O-H)$ are the deviations from the monomer. D_e is the total bond energy from the bottom of the well, and D_0 is the net bond energy from the lowest vibrational level (the quantity to be measured experimentally). Cases with errors of less than 0.005 Å, 10 cm⁻¹, and 0.1 kcal/mol are indicated in boldface. b Reference 1, CCSD(T)(FULL)/IO275 → ∞ (IO275: interaction optimized basis set with 275 basis functions for the H₂O dimer. O: 7s5p5d3f2g1h; H_d: 2s4p1d; H: 2s3p; BF: 3s3p2d1f). c Reference 24, CCSD(T)/TZ2P(f,d)+dif. Combining the best ab initio estimate for the dimer¹ with the best experimental value for the monomer²⁵ leads to $\Delta r_d(O-H) = 0.007$ Å d d d 0 corrected from the best ab initio d 0 is the measured property. d 0 was estimated by adding the zero-point energy calculated at the HF/4-21G level. g 0 and d 0 are BSSE-corrected. In all of our calculations, unscaled zero-point energies are used to convert d 0 to d 0.

Kim and Jordan reported $\beta = 59.5^{\circ}$ for B3LYP/aug-cc-pVTZ-(-f) and 56.7° for B3LYP/aug-cc-pVTZ.⁴¹ Thus, we anticipate that the inclusion of the f functions on O may bring the predicted angle β for the hybrid methods into close agreement with the best ab initio calculations.

HF/aug-cc-pVTZ(-f) gives $\beta = 49.2^{\circ}$, which is smaller than the best ab initio number by 6.5°, but LDA(SVWN) overshoots, giving $\beta = 71.9^{\circ}$, which is 16.3° too large. The various nonhybrid GGAs lead to $\beta \approx 65^{\circ}$, which is 9.4° too large.

3.2.3. Vibrational Frequencies. 3.2.3a. High-Frequency Modes. The H_2O dimer has 12 vibrational frequencies, of which 6 correspond to the high frequencies of the water monomer as modified by the presence of the other monomer. These six have been well characterized experimentally. 34,35 Table 5 summarizes both the observed frequencies (lower value) and the harmonic value deduced from the spectra (upper value). We compare the calculations to these harmonic values.

The best results are for X3LYP (MAD = 12.3 cm^{-1}) and B3LYP (MAD = 15.0 cm^{-1}). For the other hybrid methods, the MAD ranges from 21.3 to 31.5 cm⁻¹ except BH&HLYP with MAD = 115 cm^{-1} . The various nonhybrid GGA methods lead to frequencies that are too low and a MAD from 90 to 122 cm⁻¹, and LDA leads to 122 cm⁻¹. However, HF leads to vibrational frequencies that are too high with MAD = 255 cm^{-1} .

3.2.3b. Shifts in the High-Frequency Modes. It is of interest to test the ability of a variety of functionals to predict the characteristic frequency shift $\Delta \nu_{\rm d}({\rm OH})$ in the donor O–H stretching mode upon forming a hydrogen bridge. Following Bleiber and Sauer,⁴⁴ we compare the harmonic donor O–H stretching mode, $\nu_{\rm 4}$ in Table 5, of the dimer with the arithmetic mean $\bar{\nu}=(\nu_1+\nu_3)/2$ of the symmetric and asymmetric harmonic stretching modes of the free monomer in order to account for the strong coupling of these two modes in the

monomer. The experimental harmonic frequencies of the water monomer and dimer lead to $\Delta\nu_d=-170~\text{cm}^{-1}.$

The best ab initio value obtained by Tschumper et al. at CCSD(T)/TZ2P(f,d)+dif is $-138~cm^{-1}$, 24 underestimating the frequency shift by 32 cm $^{-1}$.

The best DFT results are for X3LYP and B3LYP, giving $\Delta\nu_d=-170$ and -173 cm $^{-1}$, respectively, in excellent agreement with experiment. The MAD for the eight flavors of hybrid methods is 15 cm $^{-1}$. The MAD for the seven flavors of nonhybrid GGAs examined here is 34 cm $^{-1}$. BLYP and XLYP outperform the other nonhybrid GGAs, leading to $\Delta\nu_d=-182$ and -168 cm $^{-1}$, respectively. LDA significantly overestimates this quantity, leading to $\Delta\nu_d=-364$ cm $^{-1}$, exaggerating the frequency shift by 114%.

3.2.3c. Low-Frequency Modes. The other six vibrational frequencies of the H_2O dimer are intermolecular modes, which are very anharmonic. It has not been possible to extract the harmonic frequencies from experiment, and thus for these systems, we use the best ab initio values²⁴ as the reference.

The best performance is for BH&HLYP with MAD = 2.3 cm^{-1} . PW1PW is the worst method for this quantity, leading to MAD = 35.2 cm^{-1} . The MAD for X3LYP is 8.2 cm^{-1} .

3.2.3d. Summary. Among the DFT methods, the best estimates of the important quantities relating to the water dimer, $R_{\rm e}({\rm O-O})$, $\Delta r_{\rm d}({\rm O-H})$, $\Delta \nu_{\rm d}({\rm OH})$, and $D_{\rm e}$, are given by X3LYP. These values for the various methods are summarized in Table 6.

3.3. Transition Barriers for the Interchange of Hydrogen Atoms within the Water Dimer. To understand quantitatively the rotational and vibrational spectra of the water dimer requires a knowledge of the transition barriers for the interchange of hydrogen atoms within the dimer. However, relatively few ab initio quantum mechanical studies have focused on these barriers. ^{24,45–48}

Figure 2. Transition states for the interchange of hydrogen atoms within the water dimer. The process in eq 1 is denoted acceptor H₂O rotation, the process in eq 2 is denoted donor-acceptor interchange, the process in eq 3 is denoted donor inversion, and the process in eq 4 is denoted donor-inversion-acceptor rotation.

Figure 2 shows the transition-state (TS) structures of primary interest.

- (1) Acceptor H₂O Rotation, Pathway 1. This involves an internal rotation of the acceptor water about the hydrogen bond such that two hydrogens (H₃ and H₄ in Figure 3) of the acceptor water are interchanged.
- (2) Donor-Acceptor Interchange, Pathway 2. This interchanges donor and acceptor water molecules.
- (3) Donor Inversion, Pathway 3. This interchanges the two hydrogens of the donor water (H_1 and H_2 in Figure 3).
- (4) Donor-Inversion-Acceptor Rotation, Pathway 4. This interchanges the two hydrogens of the donor water as in pathway 3 while also interchanging the two hydrogens of the acceptor water (as in Pathway 1). The transition state is TS3, just as for Pathway 3.

The best ab initio calculation available is at the CCSD(T)/ TZ2P(f,d)+diff level, accompanied by a focal point analysis (FPA) extrapolated to the complete basis set (CBS) limit in both one- and n-particle spaces.²⁴ This FPA/CBS estimate leads to²⁴

$$TS1(TS2)[TS3] = 0.52(0.70)[1.77] \text{ kcal/mol}$$

which serves as a reference to validate our DFT calculation results.

The best previous calculations with MP4/6-311+G(2df,2p)// MP2/6-311+G(d,p) led to TS1(TS2)[TS3] = 0.59(0.87)[1.88]kcal/mol.⁴⁵ An earlier study based on an empirical potential energy surface (PES) gave TS1(TS2)[TS3] = 0.4(2.3)[2.9] kcal/mol. 49 Mok et al studied the full six-dimensional intermolecular PES based on B3PW91*, where the weight of the exact exchange was increased from the standard value of 0.20 to 0.30 to obtain $R_{\rm e}({\rm O-O})$ for the water dimer close to the experimental value of 2.952 Å. B3PW91* led to barrier heights of TS1(TS2)- $[TS3] = 0.36(0.79)[1.34]^{.50}$ Other recent high-quality ab initio calculations are the following: MP2/cc-pVTZ gave TS1(TS2)-[TS3] = 0.53(0.83)[2.00], $^{46-48}$ and MP2/cc-pVQZ led to 0.52(0.79)[1.94] kcal/mol.^{46,47} An interaction optimized basis set (IOM) combined with MP2 and a counterpoise technique gave $TS1(TS2)[TS3] = 0.47(0.72)[1.92] \text{ kcal/mol.}^{48}$

TABLE 7: Barrier Heights (kcal/mol) for the Interchange of Hydrogen Atoms within the Dimer^a

,			
	C_1 , TS1	C_i , TS2	C_{2v} , TS3
HF	0.40	0.74	1.30
LDA(SVWN)	0.89	0.93	3.61
	GGA		
BLYP	0.60	1.08	2.08
BP86	0.84	1.34	2.47
BPW91	0.63	1.16	2.00
PWPW	0.67	1.05	2.29
mPWPW	0.73	1.09	2.23
PBEPBE	0.66	1.03	2.22
XLYP	0.59	1.02	2.02
Hy	brid Methods		
BH&HLYP	0.55	0.92	1.97
B3LYP	0.59	1.03	2.05
B3P86	0.66	1.13	2.26
B3PW91	0.61	1.11	1.99
PW1PW	0.63	1.01	2.12
mPW1PW	0.63	1.04	2.08
PBE1PBE	0.63	1.00	2.07
X3LYP	0.59	0.99	2.08
MP4/6-311+G(2df,2p)//	0.59	0.87	1.88
$MP2/6-311+G(d,p)^b$			
MP2/cc-pVTZ ^{c,d}	0.53	0.83	2.00
MP2/cc-pVQZ ^c	0.52	0.79	1.94
MP2/IOM CPe	0.47	0.72	1.94
FBA/CBS ^f	0.52	0.70	1.77

^a Cases with errors of less than 0.1 kcal/mol are indicated in boldface. We consider FBA/CBS to be the reference. ^b Reference 45. ^c Reference 46. d Reference 47. e Reference 48. Interaction optimized basis set of 136 functions, combined with counterpoise calculations. ^f Reference 24. Focal-point analysis extrapolated to the complete basis set limit in both one- and n-particle spaces.

Table 7 shows that all levels of theory agree that TS1 < TS2 < TS3. It has been concluded that there are 8 equivalent equilibrium structures of Figure 1 with different numberings of hydrogen atoms, 16 equivalent structures of TS1, 8 equivalent structures of TS2, and 4 equivalent structures of TS3.45 Because TS2 lies energetically below TS3, TS2 alone can achieve complete scrambling of the four hydrogen atoms within the individual water moieties, making TS3 unnecessary.

TABLE 8: Optimized Key Geometrical Parameters of (H₂O)₂ for TS1(TS2)[TS3]^a

	$R(H_1O_1)$	$R(H_1 \cdots O_2)$	$R(O_1 \cdots O_2)$	$\angle O_1H_1O_2$
HF	0.945(0.943)[0.942]	2.137(2.458)[2.707]	3.073(2.978)[3.182]	171.0(114.7)[112.0]
LDA(SVWN)	0.988(0.980)[0.973]	1.740(2.024)[2.265]	2.724(2.635)[2.761]	173.5(118.4)[110.6]
		GGA		
BLYP	0.980(0.976)[0.973]	2.001(2.335)[2.621]	2.978(2.912)[3.122]	174.3(117.2)[112.2]
BP86	0.981(0.976)[0.973]	1.960(2.262)[2.581]	2.936(2.860)[3.083]	172.2(118.6)[112.2]
BPW91	0.978(0.973)[0.970]	2.002(2.353)[2.699]	2.979(2.936)[3.202]	178.2(117.7)[112.8]
PWPW	0.979(0.974)[0.970]	1.921(2.280)[2.699]	2.900(2.864)[3.202]	177.9(117.6)[112.8]
mPWPW	0.979(0.974)[0.970]	1.938(2.280)[2.571]	2.915(2.864)[3.072]	176.4(117.6)[112.2]
PBEPBE	0.980(0.975)[0.972]	1.939(2.275)[2.547]	2.916(2.861)[3.048]	174.2(117.6)[112.1]
XLYP	0.979(0.975)[0.973]	2.003(2.346)[2.621]	2.984(2.917)[3.121]	174.4(116.7)[112.2]
		Hybrid Methods		
BH&HLYP	0.957(0.954)[0.951]	1.972 (2.293)[2.533]	2.922 (2.835)[3.014]	171.9(115.3)[111.4]
B3LYP	0.969(0.966)[0.963]	1.979(2.314)[2.574]	2.941(2.874)[3.066]	171.4(116.2)[111.8]
B3P86	0.969(0.964)[0.961]	1.926(2.263)[2.532]	2.895(2.835)[3.023]	178.7(117.1)[111.8]
B3PW91	0.968(0.964)[0.961]	1.986(2.334)[2.632]	2.953(2.900)[3.125]	177.4(116.9)[112.3]
PW1PW	0.966(0.962)[0.959]	1.936(2.279)[2.538]	2.897(2.842)[3.028]	172.9(116.5)[111.8]
mPW1PW	0.966(0.962)[0.959]	1.945(2.291)[2.563]	2.906(2.853)[3.053]	173.0(116.5)[111.9]
PBE1PBE	0.967(0.963)[0.960]	1.951(2.288)[2.543]	2.913(2.852)[3.034]	172.6(116.6)[111.8]
X3LYP	0.968(0.964)[0.962]	1.967 (2.297)[2.547]	2.926 (2.855)[3.037]	170.7(116.0)[111.7]
best ab initio ^b	0.965(0.962)[0.960]	1.972(2.370)[2.515]	2.925(2.917)[3.010]	169.0(115.6)[112.0]

^a Refer to Figure 2 for atom numbers. Distances are in Å, and angles are in degrees. Errors of less than 0.005 Å and 1° are indicated in boldface. ^b Reference 24.

Generally, hybrid methods perform slightly better than pure GGA methods. BH&HLYP has the best results, overestimating TS1 by 6%, TS2 by 31%, and TS3 by 11%. X3LYP and B3LYP also provide reasonably good results, with TS1 and TS3 overestimated by 16% (X3LYP) and 15% (B3LYP) and TS2 41% (X3LYP) and 47% (B3LYP) too high. This leads to average errors of 24% (X3LYP) and 25% (B3LYP) for the prediction of all three barriers.

Results from GGA and hybrid methods compare much more favorably with those from the ab initio calculations. XLYP is the best GGA method examined here, with TS1(TS2)[TS3] = 0.59(1.02)[2.02] kcal/mol. BLYP, BPW91, and PBEPBE provide comparable accuracies. On average, the three barrier heights are 24% (XLYP), 29% (BLYP), and 33% (BPW91 and PBEPBE) too high.

HF is too soft, leading to TS1 and TS3 values that are \sim 25% too low. However LDA(SVWN) is too much stiff, leading to barriers for TS1, TS2, and TS3 that are 71%, 33%, and 104% too high, respectively.

Table 8 summarizes the key geometric parameters for TS1-(TS2)[TS3] obtained from various levels of DFT calculations. The CCSD(T)/TZ2P(f,d)+dif results are also listed for comparison.²⁴

4. Summary

The present study reports an extensive DFT study on the ground-state properties of the water monomer and dimer, including the transition states involving the interchange of hydrogen atoms within the dimer. We considered HF, LDA-(SVWN), seven pure GGA methods (BLYP, BP86, BPW91, PWPW, mPWPW, PBEPBE, and XLYP) and eight hybrid GGA methods (BH&HLYP, B3LYP, B3P86, B3PW91, PW1PW, mPW1PW, PBE1PBE, and X3LYP). Our main results are the following:

(1) Ground-State Properties of the Water Monomer. HF gives an O–H bond length that is too short (by $0.016 \,\text{Å}$), a vibrational frequency that is too high (MAD = 237 cm⁻¹), a dipole moment that is too high (by $0.092 \,\text{D}$), and a static electric polarizability that is too low (MAD = $0.212 \,\text{Å}^3$). LDA(SVWN) generally overcorrects the HF results, leading to an O–H bond length

that is too long (by 0.013 Å), a vibrational frequency that is too low (MAD = 99 cm⁻¹), a dipole moment that is still too high (by 0.014 D), and a static electric polarizability that is too high (MAD = 0.097 ų). GGAs are *not* an improvement over LDA in predicting the ground-state properties of the water monomer. Hybrid methods (with the exception of BH&HLYP, which includes too much exact exchange) are the indisputable winners, leading to an average MAD = 0.003 Å for the O–H bond length, 16 cm^{-1} for the vibrational frequency, 0.007 D for the dipole moment, and 0.016 ų for the static electric polarizability.

- (2) Ground-State Properties of Water Dimer. HF underestimates the intermolecular hydrogen bonding, but LDA(SVWN) significantly overestimates the hydrogen bonding. Thus, HF leads to an O···O distance that is 0.136 Å too long, a donor water O-H bond elongation that is 33% too small, a shift of the donor O-H stretching that is 43% too small, and a binding energy that is 34% too small. In contrast, LDA(SVWN) leads to $R_e(O \cdot \cdot \cdot O)$ that is 0.202 Å too short, $\Delta r_d(OH)$ that is 217% too large, $\Delta \nu_{\rm d}({\rm OH})$ that is 114% too high, and $D_{\rm e}$ that is 80% too large. GGA shows significant improvement over LDA-(SVWN). On average, GGAs leads to MAD = 0.025 Å for $R_{\rm e}({\rm O\cdots O}), \, \Delta r_{\rm d}({\rm OH})$ that is 83% too large, and $\Delta \nu_{\rm d}({\rm OH})$ that is 24% too large, with the exception of XLYP, whose $\Delta \nu_d(OH)$ is slightly smaller (by 1%). GGAs give D_e values ranging from 3.60 (BPW91) to 5.43 (PWPW), with PBEPBE being the best for this quality. Hybrid methods are again the winners, leading to results comparable to the best ab initio results. The best hybrid method is X3LYP, which consistently gives the best estimations of $R_e(O-O)$, $\Delta r_d(O-H)$, $\Delta \nu_d(OH)$, and D_e .
- (3) Transition Barriers for Interchange of Hydrogen Atoms in the Water Dimer. HF underestimates the barrier heights, but LDA(SVWN) overestimates the barrier heights. GGAs with or without including exact exchange lead to barrier heights that compare well with MP2 results with basis sets of similar size. XLYP is the best pure GGA, and BH&HLYP is the best hybrid method for the prediction of the transition barrier.

Considering all of these factors, we find that X3LYP provides the best overall description of the properties of the water dimer,

making it the method of choice for examining other hydrogenbonded systems.

Acknowledgment. This research was funded partially by NSF (CHE 9985574) and by NIH (HD 36385-02). The facilities of the Materials and Process Simulation Center used in these studies were funded by ARO-DURIP, ONR-DURIP, NSF-MRI, a SUR Grant from IBM, and the Beckman Institute. In addition, the Materials and Process Simulation Center is funded by grants from DOE-ASCI, ARO-MURI, ONR-MURI, ONR-DARPA, NIH, NSF, General Motors, ChevronTexaco, Seiko-Epson, and. Asahi Kasei.

References and Notes

- (1) Klopper, W.; van Duijneveldt-van de Rijdt, J. G. C. M.; van Duijneveldt, F. B. Phys. Chem. Chem. Phys. 2000, 2, 2227
- (2) Xu, X.; Goddard, W. A., III Proc. Natl. Acad. Sci. USA 2004, 101, 2673.
 - Slater, J. C. Phys. Rev. 1951, 81, 385. (3)
 - (4) Vosko, S. H.; Wilk, L.; Nusair, M. Can. J. Phys. 1988, 58, 1200.
 - (5) Lee, C. T.; Yang, W. T.; Parr, R. G. Phys. Rev. B 1988, 37, 785.
 - (6) Becke, A. D. J. Chem. Phys. 1993, 98, 5648.
 - (7) Becke, A. D. Phys. Rev. A 1988, 38, 3098.
 - (8) Perdew, J. P.; Wang, Y. Phys. Rev. B 1986, 33, 8800.
 - (9) Perdew, J. P.; Zunger, A. Phys. Rev. B 1981, 23, 5048.
- (10) Perdew, J. P. In Electronic Structure Theory of Solids; Ziesche, P., Eschrig, H., Eds.; Akademie Verlag: Berlin, 1991; p11.
 - (11) Perdew, J. P.; Wang, Y. Phys. Rev. B 1992, 45, 13244.
 (12) Adamo, C.; Barone, V. J. Chem. Phys. 1998, 108, 664.
- (13) Perdew, J. P.; Burke, K.; Ernzerhof, M. Phys. Rev. Lett. 1996, 77,
 - (14) Ernzerhof, M.; Scuseria, G. E. J. Chem. Phys. 1999, 110, 5029.
 - (15) Pérez-Jordá, J. M.; Beck, A. D. Chem. Phys. Lett. 1995, 233, 134.
 - (16) Kristyan, S.; Pulay, P. Chem. Phys. Lett. 1994, 229, 175
- (17) Goldman, N.; Fellers, R. S.; Brown, M. G.; Braly, L. B.; Keoshian, C. J.; Leforestier, C.; Saykally, R. J. J. Chem. Phys. 2002, 116, 10148.
- (18) Jaguar 4.0; Schrödinger Inc.: Portland, OR, 2000.
- (19) Dunning, T. H., Jr. J. Chem. Phys. 1989, 90, 1007.
- (20) Kendall, R. A.; Dunning, T. H., Jr.; Harrison, R. J. J. Chem. Phys. 1992, 96, 6796.
- (21) Simon, S.; Duran, M.; Dannenberg, J. J. J. Phys. Chem. A 1999, 103, 1640.

- (22) Halkier, A.; Koch, H.; Jorgensen, P.; Christiansen, O.; Nielsen, I. M. B.; Helgaker, T. Theor. Chem. Acc. 1997, 97, 150.
 - (23) Boys, S. F.; Bernardi, F. Mol. Phys. 1970, 19, 553.
- (24) Tschumper, G. S.; Leininger, M. L.; Hoffman, B. C.; Waleev, E. F.; Schaefer, H. F., III; Quack, M. J. Chem. Phys. 2002, 116, 690.
- (25) Benedict, W. S.; Gailan, N.; Plyler, E. K. J. Chem. Phys. 1956, *24*, 1139.
 - (26) Hoy, A. R.; Bunker, P. R. J. Mol. Spectrosc. 1975, 59, 159.
- (27) Cook, R. L.; de Lucia, F. C.; Helminger, P. J. Mol. Spectrosc. **1975**, 53, 62,
 - (28) Kuchitsu, K.; Morino, Y. Bull. Chem. Soc. Jpn. 1965, 38, 1521.
 - (29) Dyke, T. R.; Muenter, J. S. J. Chem. Phys. 1973, 59, 1325.
 - (30) John, I. J.; Backsay, G. B.; Hush, N. S. Chem. Phys. 1980, 51, 49.
 - (31) Murphy, W. F. J. Chem. Phys. 1977, 67, 5877.
- (32) Koch, W.; Holthausen, M. C. A Chemist's Guide to Density Functional Theory; Wiley-VCH: Weinheim, Germany, 2000; pp 217-226.
 - (33) Odutola, J. A.; Dyke, T. R. J. Chem. Phys. 1980, 72, 5062.
- (34) Fredin, L.; Nelander, B.; Ribbegard, G. J. Chem. Phys. 1977, 66, 498
 - Nelander, B. J. Chem. Phys. 1978, 69, 3870. (35)
- (36) Bentwood, R. M.; Barnes, A. J.; Orville-Thomas, W. J. J. Mol. Spectrosc. 1980, 84, 391.
- (37) Tursi, A. J.; Nixon, E. R. J. Chem. Phys. 1970, 52, 1521.
- (38) Curtiss, L. A.; Frurip, D. J.; Blander, M. J. Chem. Phys. 1979, 71,
- (39) Feyerersen, M. W.; Feller, D.; Dixon, D. A. J. Phys. Chem. 1996, 100, 2993.
- (40) Estrin, D. A.; Paglieri, L.; Corongiu, G.; Clementi, E. J. Phys. Chem. 1996, 100, 8701.
 - (41) Kim, K.; Jordan, K. D. J. Phys. Chem. 1994, 98, 10089.
- (42) Hobza, P.; Bludsky, O.; Suhai, S. Phys. Chem. Chem. Phys. 1999, 1, 3073.
- (43) Frisch, M. J.; Del Bene, J. E.; Binkley, J. S.; Schaefer, H. F., III J. Chem. Phys. 1986, 84, 2279.
 - (44) Bleiber, A.; Sauer, J. Chem. Phys. Lett. 1995, 238, 243.
- (45) Smith, B. J.; Swanton, D. J.; Pople, J. A.; Schaefer, H. F., III; Radom, L. J. Chem. Phys. 1990, 92, 2401.
 - (46) Taketsugu, T.; Wales, D. J. Mol. Phys. 2002, 100, 2793.
 - (47) Burnham, C. J.; Xantheas, S. S. J. Chem. Phys. 2002, 116, 1479.
- (48) van Duijneveldt-van de Rijdt, J. G. C. M.; Mooij, W. T. M.; van Duijneveldt, F. B. Phys. Chem. Chem. Phys. 2003, 5, 1169.
 - (49) Coudert, L. H.; Hougen, J. T. J. Mol. Spectrosc. 1988, 130, 86.
- (50) Mok, D. K. W.; Handy, N. C.; Amos, R. D. Mol. Phys. 1997, 92, 667.